Available online at www.sciencedirect.com
ScienceDirect
Trans. Nonferrous Met. Soc. China 26(2016) 791−798
Transactions of Nonferrous Metals Society of China
www.tnmsc.cn

Effects of Ti-based additives on Mg_2FeH_6 dehydrogenation properties

Chen-chen XU, Xue-zhang XIAO, Jie SHAO, Lang-xia LIU, Teng QIN, Li-xin CHEN

State Key Laboratory of Silicon Materials, Key Laboratory of Advanced Materials and Applications for Batteries of Zhejiang Province, School of Materials Science and Engineering, Zhejiang University, Hangzhou 310027, China

Received 6 January 2015; accepted 4 April 2015

Abstract: Mg_2FeH_6 doped with and without Ti and its alloys ($TiMn_2$, TiAl) were prepared combing ball milling and heat treatment. The effects of these additives on the dehydrogenation performance of Mg_2FeH_6 were studied systematically. The results show that all additives have favor influence on improving the hydrogen desorption property of Mg_2FeH_6. Especially, $TiMn_2$ exhibits prominent effect on enhancing the dehydrogenation kinetics of Mg_2FeH_6. Moreover, the activation energy of $TiMn_2$-doped Mg_2FeH_6 calculated by Kissinger equation is 94.87 kJ/mol, which is 28 kJ/mol lower than that of the undoped Mg_2FeH_6. The cycling tests suggest that the improved dehydrogenation kinetics of Mg_2FeH_6 doped by $TiMn_2$ can maintain in the second cycle.

Key words: Mg_2FeH_6; Ti-based additives; dehydrogenation properties; kinetics

1 Introduction

Hydrogen is a promising energy carrier by virtue of its abundance, high energy density as well as its environmentally friendly property [1−4]. Yet the development of safe and efficient hydrogen storage materials is of vital importance to realize the so-called hydrogen economy [2]. Complex transitional metal hydrides, especially the Mg-based 3D-transitional metal hydrides are considered to be potential candidates as hydrogen storage materials, thus attracting much interest [5−9]. Among these, Mg_2FeH_6 possesses a volumetric hydrogen density of 150 kg/m^3, which is the highest one so far. Additionally, Mg_2FeH_6 has an advantage of a larger gravimetric hydrogen density (5.47%, mass fraction) over others belonging to the same group, like Mg_2NiH_4 (3.6%), Mg_2CoH_5 (4.5%). However, the difficulties to prepare pure Mg_2FeH_6 resulting from the absence of the stable intermetallic compound between Mg and Fe hampered the deep study of Mg_2FeH_6, not to speak of the technique used to optimize its hydrogen storage properties.

In 1984, DIDISHEIM et al [10] firstly synthesized Mg_2FeH_6 through sintering under high pressure. Afterwards, a series of investigations relating to its synthesis were conducted [11−24], and the result turns out to be encouraging. While the reports regarding to the hydrogen storage properties indicated that further efforts are needed to improve the high sorption temperature and the sluggish kinetics. Strategies [25−28] including nanosizing, catalyzing, alloying and so forth seem to be effective in improving the properties of Mg-based hydrogen storage materials. To enhance the kinetics, additives usage has been widely applied. The effective additives reported mainly include transition metals, transition metal oxides and intermetallic compounds. Among the transition metals, Ti and its oxide exhibited superior catalytic effects on desorption and absorption properties [29]. ZHOU et al [30] studied the effects of Ti intermetallic catalysts on the hydrogen storage properties of MgH_2 and the results showed significant progress on the properties of MgH_2. In this work, we investigated the effect of Ti-based additives including $TiMn_2$, TiAl and Ti on the hydrogen desorption properties of Mg_2FeH_6. The in-situ adjunction of 5% (mole fraction) additives was adopted in the doping process. The hydrogen desorption properties were characterized by differential scanning calorimetry (DSC) and Sieverts apparatus. The activation energy was calculated via Kissinger equation. The

Foundation item: Project (2010CB631300) supported by the National Basic Research Program of China; Project (2012AA051503) supported by the National High Technology Research & Development Program of China; Projects (51001090, 51171173) supported by the National Natural Science Foundation of China; Project (IRT13037) supported by the Program for Innovative Research Team in University of Ministry of Education of China

Corresponding author: Xue-zhang XIAO ; Tel: +86-571-87951876; Fax: +86-571-87951152; E-mail: xzxiao@zju.edu.cn

DOI: 10.1016/S1003-6326(16)64169-9

consequence shows that $TiMn_2$ exhibits better catalytic effects over the others. The dehydrogenation reaction mechanism was also investigated.

2 Experimental

Mg (purity, 98%) and Ti powders (purity, 99%) were purchased from Sinopharm Chemical Reagent Co. Ltd., China. Fe (purity, 98%) was purchased from Shanghai Jinshan Smelter, China. $TiMn_2$ and TiAl alloys were prepared by suspension induction melting firstly, and then the as-prepared alloys were ball-milled for 4 h under 4 MPa H_2 atmosphere.

The mixtures with n(Mg):n(Fe):n(TMs) (TMs= $TiMn_2$, TiAl, Ti) of 2.2:1:0.05 were ball-milled for 20 h in a planetary mill under 4 MPa H_2. Hereafter, heat treatment was conducted at 500 ℃ for 40 h under 9 MPa H_2 for the ball-milled mixtures. Finally, all the samples were ball-milled for 5 h under 2 MPa H_2 atomosphere. All the materials handling was carried out in the glovebox filled with argon to prevent the pollution from H_2O and O_2.

The structural analysis of the sample was conducted by X-ray diffraction (XRD). The differential scanning calorimetry (DSC) was executed on a Netzsch STA 449F3 instrument heating from 30 to 450 ℃ under the continuous protective gas of argon with heating rates of 2, 5, 10 ℃/min, respectively. Hydrogen desorption properties of the samples were examined combining temperature-programmed desorption (TPD) and isothermal desorption tests via a Sievert apparatus. To compare the hydrogen capacity of Mg_2FeH_6 directly, the TMs content was not taken into account in the determination of hydrogen desorption process.

3 Results and discussion

3.1 Characterization of samples

Figure 1 shows the XRD patterns of as-prepared Mg_2FeH_6 doped with and without TMs. The inset shows that $TiMn_2$ and TiAl were synthesized. According to the results, no distinct differences exist among the samples. All samples exhibit strong diffraction peaks of Mg_2FeH_6 with some residual Fe phase, which may be a result of the decomposition during the final 5 h ball-milling. Meanwhile, the existing MgO phase could result from the contamination during the XRD detection. Moreover, no TMs additives phases exist in the XRD pattern. It could result from the relatively less quantities added [22].

3.2 Hydrogen desorption properties of samples

Figure 2 displays the hydrogen desorption properties of as-prepared Mg_2FeH_6 doped with and

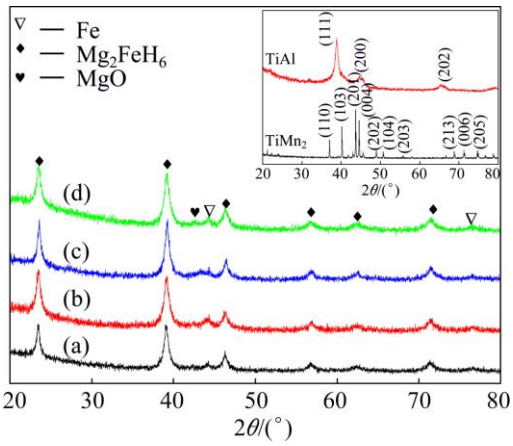

Fig. 1 XRD patterns of as-prepared Mg_2FeH_6 (a) and Mg_2FeH_6 doped with $TiMn_2$ (b), TiAl (c) and Ti (d)

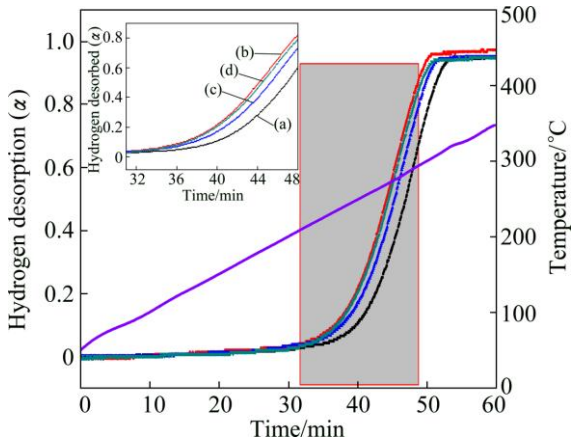

Fig. 2 TPD curves of Mg_2FeH_6 (a), and Mg_2FeH_6 doped with $TiMn_2$ (b), TiAl (c) and Ti (d) conducted at 5 ℃ /min to 450 ℃ under 100 Pa H_2

without TMs measured by TPD conducted at a heating rate of 5 ℃/min. It is obviously found that both the onset and offset hydrogen desorption temperatures of Mg_2FeH_6 doped with TMs decrease compared with those of undoped Mg_2FeH_6. The hydrogen desorption of TMs doped samples starts from 200 ℃, nearly 20 ℃ lower than that of undoped Mg_2FeH_6, suggesting improved dehydrogenation properties. Moreover, $TiMn_2$ exhibits best performance in improving the dehydrogenation of Mg_2FeH_6, followed by Ti and TiAl. Given the similar crystalline size in Fig. 1 and similar particle size after ball-milling shown in Fig. 3, it is believed that the differences among dehydrogenation properties for the TMs doped samples derive from the differences of the catalytic component. The theoretical hydrogen released for the Mg_2FeH_6, Mg_2FeH_6−$TiMn_2$, Mg_2FeH_6−TiAl, Mg_2FeH_6−Ti are 5.47%, 5.08%, 5.3% and 5.34% (mass fraction), respectively, and the actual hydrogen amount released is over 95% of the total hydrogen storage capacity, which are 5.20%, 4.83%, 5.04% and 5.07%

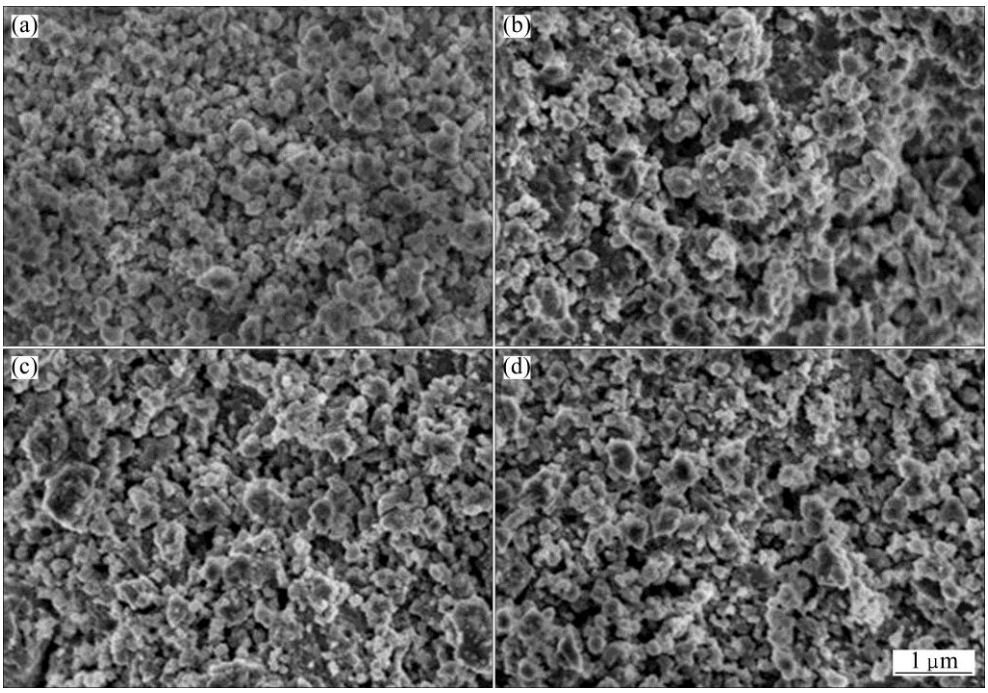

Fig. 3 SEM images of Mg_2FeH_6 (a), and Mg_2FeH_6 doped with $TiMn_2$ (b), TiAl (c) and Ti (d)

(mass fraction), respectively. This manifests the high purity of Mg_2FeH_6 which agrees well with the results of XRD patterns.

In addition, the isothermal hydrogen desorption tests of Mg_2FeH_6 doped with and without TMs were carried out at 260 ℃ under 100 Pa H_2, as shown in Fig. 4. All samples show favor hydrogen desorption kinetics. At a temperature as low as 260 ℃, all samples could release 75% H_2 in 30 min. As expected, the Mg_2FeH_6 doped with $TiMn_2$ shows the best dehydrogenation performance among the samples, whose dehydrogenation rate is nearly two times faster than that of the undoped Mg_2FeH_6.

To further understand the improved kinetics by calculating the activation energy, the DSC experiment

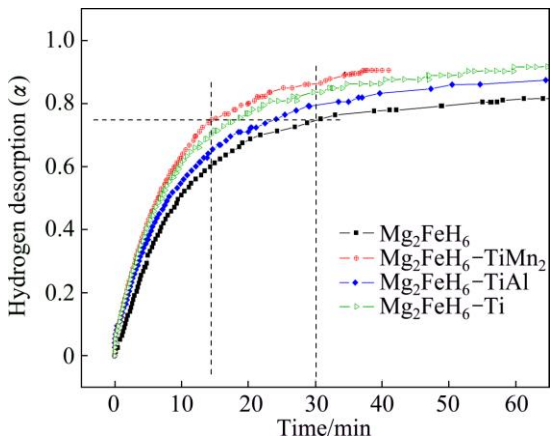

Fig. 4 Isothermal hydrogen desorption curves at 260 ℃ under 100 Pa H_2

was conducted by heating up to 450 ℃ with the heating rates of 2, 5, 10 ℃/min, respectively. Figure 5 shows the DSC profiles of Mg_2FeH_6 doped with and without TMs. Each curve presents one endothermic peak indicating the one-step dehydrogenation of Mg_2FeH_6, as manifested in the previous reports [21,31]. Table 1 presents the peak temperatures relevant to the DSC consequences. For Mg_2FeH_6 doped with 5% $TiMn_2$, the dehydrogenation peak temperature is 266.9 ℃, nearly 25 ℃ lower than that of the as-prepared Mg_2FeH_6, thus, the result is in good agreement with the TPD results.

The activation energy of the hydrogen desorption process can be estimated according to the Kissinger equation [32]:

$$\frac{\mathrm{d}\left(\ln\dfrac{\beta}{T_\mathrm{p}^2}\right)}{\mathrm{d}\left(\dfrac{1}{T_\mathrm{p}}\right)}=-\frac{E_\mathrm{a}}{R} \tag{1}$$

where T_p is the peak temperature corresponding to the heating rate β, E_a is the activation energy and R is the gas constant. By plotting $1000/T_\mathrm{p}$ against $\ln(\beta/T_\mathrm{p}^2)$, E_a can be obtained, as shown in Fig. 6. The activation energies of as-prepared Mg_2FeH_6 doped with and without TMs calculated according to Eq. (1) are list in Table 1. For the as-prepared Mg_2FeH_6, the activation energy is estimated as 123.48 kJ/mol, while the activation energies are 94.87, 107.66 and 97.93 kJ/mol for the Mg_2FeH_6 doped with $TiMn_2$, TiAl and Ti, respectively. The result indicates that the addition of TMs reduces the activation

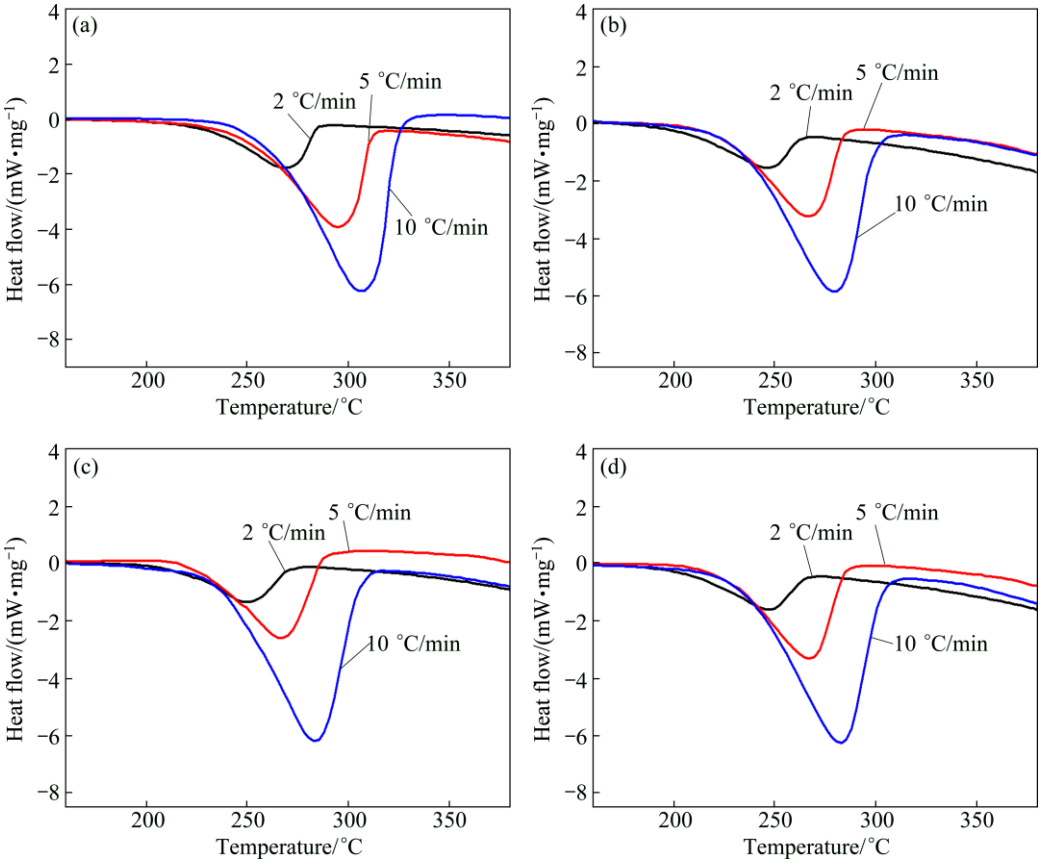

Fig. 5 DSC profiles of Mg_2FeH_6 (a), and Mg_2FeH_6 doped with $TiMn_2$ (b), TiAl (c) and Ti (d)

Table 1 Peak temperatures of DSC profiles and calculated activation energy

Alloy	Peak temperature/ ℃			E_a/(kJ·mol^{-1})
	2 ℃/min	5 ℃/min	10 ℃/min	
Mg_2FeH_6	274.8	294.2	306.5	123.48
Mg_2FeH_6−$TiMn_2$	246	266.9	283.2	94.87
Mg_2FeH_6−TiAl	250.3	267.1	283.4	107.66
Mg_2FeH_6−Ti	246.8	267.6	283.6	97.93

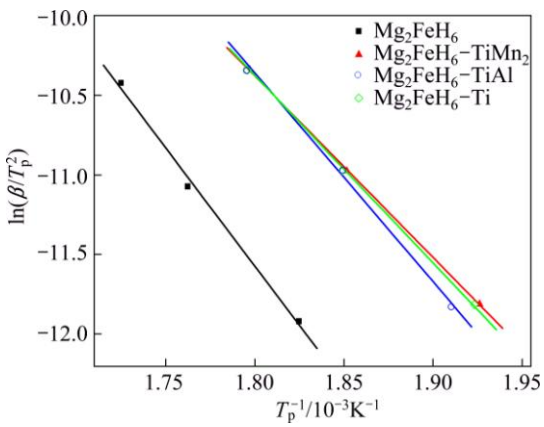

Fig. 6 Kissinger plots of Mg_2FeH_6, and Mg_2FeH_6 doped with $TiMn_2$, TiAl and Ti

energy, thus improving the dehydrogenation kinetics, among which $TiMn_2$ is the most efficient catalyst.

To investigate the kinetic mechanism of the hydrogen desorption process, isothermal dehydrogenation kinetic analysis was executed in the range of 270−300 ℃, as shown in Fig. 7. As $TiMn_2$ exhibited the best performance among the samples, this sample was used to select a most fitting model. Jone's method [33] is a widely used one in the rapid model selection. $(t/t_{0.5})_{theo}$ is constant for a certain model when t is defined, where t is the time and $t_{0.5}$ is the time when the fraction α is 0.5. The theoretical value $(t/t_{0.5})_{theo}$ closest to the experimental value $(t/t_{0.5})_{exp}$ is the most reliable model. Therefore, we plot the $(t/t_{0.5})_{exp}$ against the $(t/t_{0.5})_{theo}$ and the fitting linear slope closest to 1 is the reliable model. Figure 8 shows the relationship between the $(t/t_{0.5})_{exp}$ and the $(t/t_{0.5})_{theo}$ of the nine kinetic mechanisms, which is also listed in Table 2. From the curves, we found out that the model best fitting the hydrogen desorption is the F1 model, implying that the hydrogen desorption was controlled by the concentration of reactant. To further

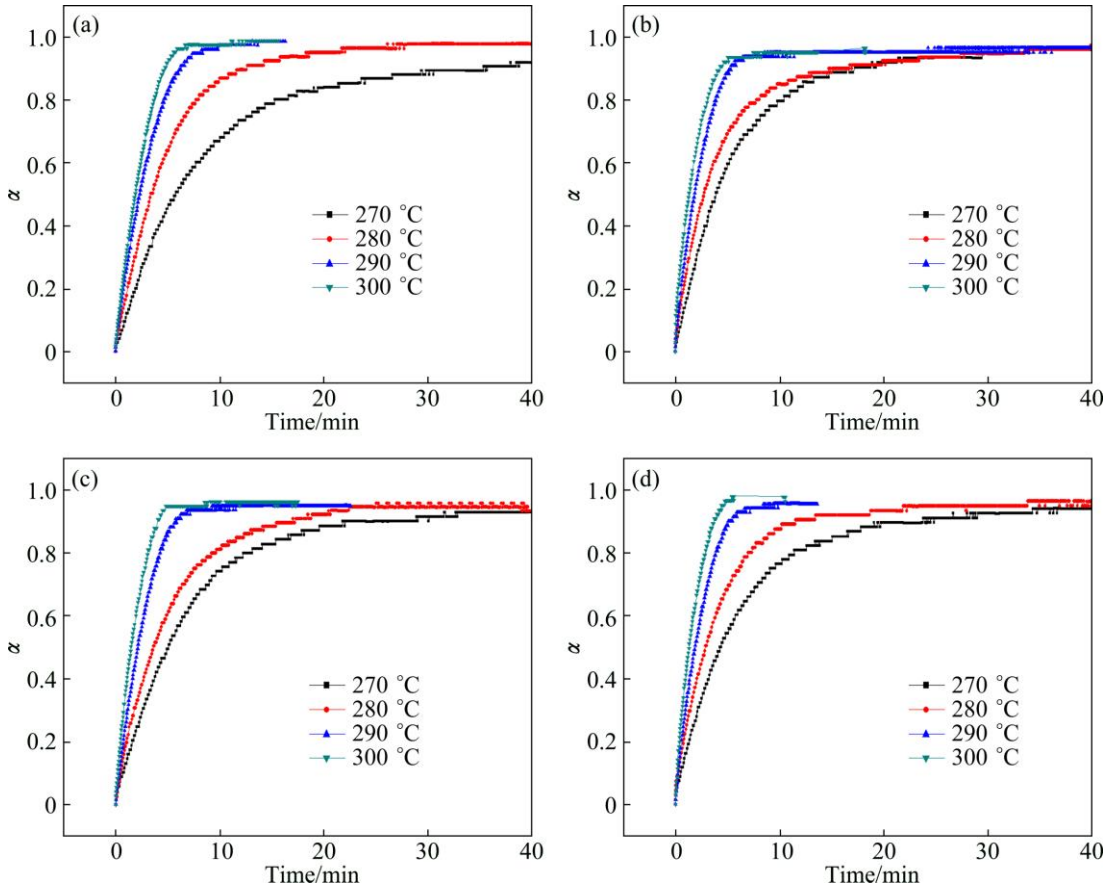

Fig. 7 Isothermal dehydrogenation curves of Mg_2FeH_6 (a), and Mg_2FeH_6 doped with $TiMn_2$ (b), TiAl (c) and Ti (d)

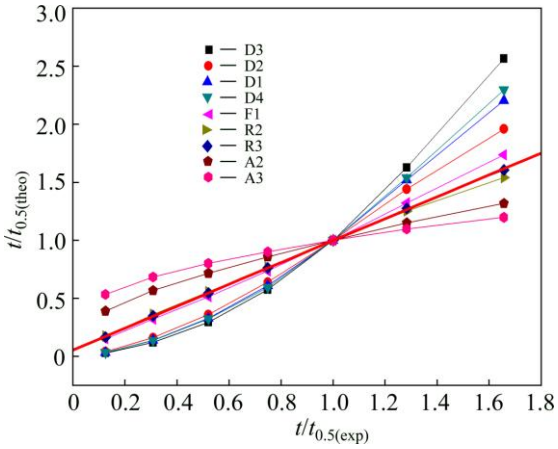

Fig. 8 $(t/t_{0.5})_{theo}$ vs $(t/t_{0.5})_{exp}$ for $TiMn_2$-doped Mg_2FeH_6 at 290 ℃

verify the model, the time dependence of F1 model was used at different temperatures with the fraction α ranging from 0.1 to 0.7 (Fig. 9) and other three samples were tested using this model. It is clearly seen that the linear coefficient R^2 for all samples are larger than 0.99, signifying the same reaction mechanism.

Considering that the $TiMn_2$ exhibits the best performance among the TMs additives in improving the dehydrogenation of Mg_2FeH_6, we investigate the reversibility of the undoped and $TiMn_2$-doped Mg_2FeH_6. The isothermal dehydrogenation was performed at 300 ℃ under 100 Pa H_2. Here, the dehydrogenation performance was employed to replace the hydrogen absorption property given that little change in temperature could bring about huge variation in pressure under high pressure [34]. Figure 10 shows the

Table 2 Kinetic models examined in isothermal desorption curves

Symbol	Model	Integral $f(\alpha)$ form	R^2
D1	One-dimensional diffusion	α^2	1.6565
D2	Two-dimensional diffusion	$\alpha+(1-\alpha)\ln(1-\alpha)$	1.2888
D3	Three-dimensional diffusion (Jander equation)	$[1-(1-\alpha)^{1/3}]^2$	1.4424
D4	Three-dimensional diffusion (Ginstling−Braunshtein equation)	$(1-2\alpha/3)-(1-\alpha)^{2/3}$	1.4935
F1	First-order reaction	$-\ln(1-\alpha)$	1.0354
R2	Two-dimensional phase	$1-(1-\alpha)^{1/2}$	0.8975
R3	Three-dimensional phase	$1-(1-\alpha)^{1/3}$	0.9435
A2	Avarami−Erofe'ev	$[-\ln(1-\alpha)]^{1/2}$	0.5947
A3	Avarami−Erofe'ev	$[-\ln(1-\alpha)]^{1/3}$	0.4211

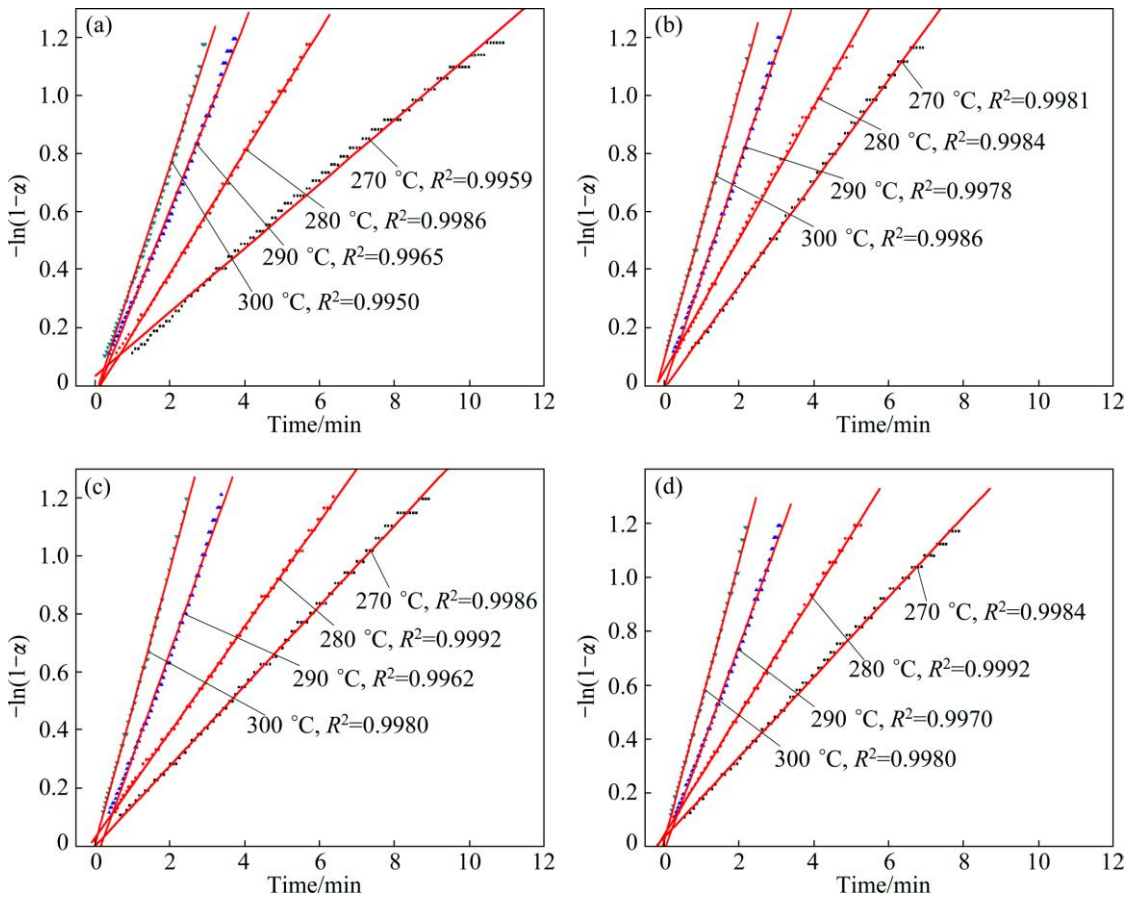

Fig. 9 Time dependence of F1 model at different temperatures for Mg_2FeH_6 (a), and Mg_2FeH_6 doped with $TiMn_2$ (b), TiAl (c) and Ti (d)

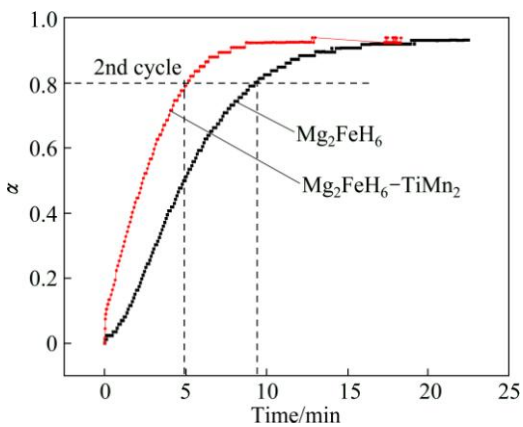

Fig. 10 Hydrogen desorption curves of Mg_2FeH_6 (a) and Mg_2FeH_6 doped with $TiMn_2$ (b) at 300 ℃ after rehydrogenation

dehydrogenation performance of the undoped and $TiMn_2$-doped Mg_2FeH_6. Obviously, both composites can release over 90% H_2 which comes from the decomposition of Mg_2FeH_6 and the residual MgH_2. Remarkably, $TiMn_2$-doped Mg_2FeH_6 releases 80% H_2 in 5 min, whereas the undoped one needs 10 min. The results imply that $TiMn_2$ can help to sustain the cycle stability of dehydrogenation kinetics of Mg_2FeH_6.

4 Conclusions

1) This research indicates that the TMs additives ($TiMn_2$, TiAl and Ti) show favor catalytic effects on improving the dehydrogenation properties of Mg_2FeH_6.

2) Particularly, the Mg_2FeH_6 doped with $TiMn_2$ exhibits the best desorption performance. The starting dehydrogenation temperature is reduced by 20 ℃ and the activation energy is decreased by 28 kJ/mol for the $TiMn_2$ doped Mg_2FeH_6 compared with that for the undoped Mg_2FeH_6.

3) The dehydrogenation mechanism was investigated as the first-order reaction model, implying that the hydrogen desorption was controlled by the concentration of reactant.

4) Moreover, the $TiMn_2$-doped Mg_2FeH_6 shows the best dehydrogenation kinetics stability during dehydrogenation cycle.

References

[1] EDWARDS P, KUZNETSOV V, DAVID W. Hydrogen energy [J].

Philosophical Transactions of the Royal Society A: Mathematical, Physical and Engineering Sciences, 2007, 365(1853): 1043−1056.

[2] SCHLAPBACH L, ZÜTTEL A. Hydrogen-storage materials for mobile applications [J]. Nature, 2001, 414 (6861): 353−358.

[3] van den BERG A W, AREÁN C O. Materials for hydrogen storage: Current research trends and perspectives [J]. Chemical Communications, 2008, 6(6): 668−681.

[4] YANG J, SUDIK A, WOLVERTON C, SIEGEL D J. High capacity hydrogen storage materials: Attributes for automotive applications and techniques for materials discovery [J]. Chemical Society Reviews, 2010, 39(2): 656−675.

[5] BOBET J, AKIBA E, NAKAMURA Y, DARRIET B. Study of Mg−M (M=Co, Ni and Fe) mixture elaborated by reactive mechanical alloying—Hydrogen sorption properties [J]. International Journal of Hydrogen Energy, 2000, 25(10): 987−996.

[6] DORNHEIM M, DOPPIU S, BARKHORDARIAN G, BOESENBERG U, KLASSEN T, GUTFLEISCH O, BORMANN R. Hydrogen storage in magnesium-based hydrides and hydride composites [J]. Scripta Materialia, 2007, 56(10): 841−846.

[7] HUOT J, PELLETIER J, LIANG G, SUTTON M, SCHULZ R. Structure of nanocomposite metal hydrides [J]. Journal of Alloys and Compounds, 2002, 330: 727−731.

[8] SAKINTUNA B, LAMARI-DARKRIM F, HIRSCHER M. Metal hydride materials for solid hydrogen storage: A review [J]. International Journal of Hydrogen Energy, 2007, 32(9): 1121−1140.

[9] ORIMO S, FUJII H. Materials science of Mg−Ni-based new hydrides [J]. Applied Physics A, 2001, 72(2): 167−186.

[10] DIDISHEIM J, ZOLLIKER P, YVON K, FISCHER P, SCHEFER J, GUBELMANN M, WILLIAMS A. Dimagnesium iron (II) hydride, Mg_2FeH_6, containing octahedral FeH_6^{4-} anions [J]. Inorganic Chemistry, 1984, 23(13): 1953−1957.

[11] GENNARI F, CASTRO F, ANDRADE GAMBOA J. Synthesis of Mg_2FeH_6 by reactive mechanical alloying: Formation and decomposition properties [J]. Journal of Alloys and Compounds, 2002, 339(1): 261−267.

[12] HUOT J, HAYAKAWA H, AKIBA E. Preparation of the hydrides Mg_2FeH_6 and Mg_2CoH_5 by mechanical alloying followed by sintering [J]. Journal of Alloys and Compounds 1997, 248(1): 164−167.

[13] LEIVA D R, de SOUZA VILLELA A C, PAIVA-SANTOS C D O, FRUCHART D, MIRAGLIA S, ISHIKAWA T T, BOTTA W J. High-yield direct synthesis of Mg_2FeH_6 from the elements by reactive milling [J]. Solid State Phenomena, 2011, 170: 259−262.

[14] NIAZ N, AHMAD I, KHALID N, AHMED E, ABBAS S, JABEEN N. Preparation of Mg_2FeH_6 nanoparticles for hydrogen storage properties [J]. Journal of Nanomaterials, 2013, 2013: 610642.

[15] POLANSKI M, PŁOCIŃSKI T, KUNCE I, BYSTRZYCKI J. Dynamic synthesis of ternary Mg_2FeH_6 [J]. International Journal of Hydrogen Energy, 2010, 35(3): 1257−1266.

[16] RETUERTO M, SÁNCHEZ-BENÍTEZ J, RODRÍGUEZ-CAÑAS E, SERAFINI D, ALONSO J. High-pressure synthesis of Mg_2FeH_6 complex hydride [J]. International Journal of Hydrogen Energy, 2010, 35(15): 7835−7841.

[17] SAI RAMAN S, DAVIDSON D, BOBET J L, SRIVASTAVA O. Investigations on the synthesis, structural and microstructural characterizations of Mg-based K_2PtCl_6 type (Mg_2FeH_6) hydrogen storage material prepared by mechanical alloying [J]. Journal of Alloys and Compounds, 2002, 333(1): 282−290.

[18] SELVAM P, YVON K. Synthesis of Mg_2FeH_6, Mg_2CoH_5 and Mg_2NiH_4 by high-pressure sintering of the elements [J]. International Journal of Hydrogen Energy, 1991, 16(9): 615−617.

[19] VARIN R, LI S, CALKA A, WEXLER D. Formation and environmental stability of nanocrystalline and amorphous hydrides in the 2Mg−Fe mixture processed by controlled reactive mechanical alloying (CRMA) [J]. Journal of Alloys and Compounds, 2004, 373(1): 270−286.

[20] WANG Yan, CHENG Fang-yi, LI Chun-sheng, TAO Zhan-liang, CHEN Jun. Preparation and characterization of nanocrystalline Mg_2FeH_6 [J]. Journal of Alloys and Compounds, 2010, 508(2): 554−558.

[21] ZHANG Xuan-zhou, YANG Rong, QU Jiang-lan, ZHAO Wei, XIE Lei, TIAN Wen-huai, LI Xing-guo. The synthesis and hydrogen storage properties of pure nanostructured Mg_2FeH_6 [J]. Nanotechnology, 2010, 21(9): 095706.

[22] LI Song-lin, TANG Sheng-long, LIU Yi, PENG Shu-ke, CUI Jian-min. Synthesis of nanostructured Mg_2FeH_6 hydride and hydrogen sorption properties of complex [J]. Transactions of Nonferrous Metals Society of China, 2010, 20(12): 2281−2288.

[23] LI S L, VARIN R A. Structural and hydrogen storage capacity evolution of Mg_2FeH_6 hydride synthesized by reactive mechanical alloying [J]. Transactions of Nonferrous Metals Society of China, 2004, 14(4): 649−653.

[24] MA Jian-li, WANG Yan, TAO Zhan-liang, CHEN Jun. Preparation and hydrogen storage properties of Mg_2FeH_6 nanocrystals [J]. Chemical Journal of Chinese Universities, 2012, 33(3): 536−540. (in Chinese)

[25] JEON K J, MOON H R, RUMINSKI A M, JIANG B, KISIELOWSKI C, BARDHAN R, URBANJ J. Air-stable magnesium nanocomposites provide rapid and high-capacity hydrogen storage without using heavy-metal catalysts [J]. Nature Materials, 2011, 10(4): 286−290.

[26] LIU Guang, WANG Yi-jing, QIU Fang-yuan, LI Li, JIAO Li-fang, YUAN Hua-tang. Synthesis of porous Ni@ rGO nanocomposite and its synergetic effect on hydrogen sorption properties of MgH_2 [J]. Journal of Materials Chemistry, 2012, 22(42): 22542−22549.

[27] MALKA I, CZUJKO T, BYSTRZYCKI J. Catalytic effect of halide additives ball milled with magnesium hydride [J]. International Journal of Hydrogen Energy, 2010, 35(4): 1706−1712.

[28] ZHANG J, CUEVAS F, ZAÏDI W, BONNET J P, AYMARD L, BOBET J L, LATROCHE M. Highlighting of a single reaction path during reactive ball milling of Mg and TM by quantitative H_2 gas sorption analysis to form ternary complex hydrides (TM= Fe, Co, Ni) [J]. The Journal of Physical Chemistry C, 2011, 115(11): 4971−4979.

[29] PAN Yin-cheng, ZOU Jian-xin, ZENG Xiao-qin, DING Wen-jiang. Hydrogen storage properties of Mg−TiO_2 composite powder prepared by arc plasma method [J]. Transactions of Nonferrous Metals Society of China, 2014, 24(12): 2834−3839.

[30] ZHOU Cheng-shang, FANG Zhi-gang, REN Chai, LI Jing-zhu, LU Jun. Effect of Ti intermetallic catalysts on hydrogen storage properties of magnesium hydride [J]. The Journal of Physical Chemistry C, 2013, 117(25): 12973−12980.

[31] PUSZKIEL J, ARNEODO LAROCHETTE P, GENNARI F. Thermodynamic–kinetic characterization of the synthesized Mg_2FeH_6−MgH_2 hydrides mixture [J]. International Journal of Hydrogen Energy, 2008, 33(13): 3555−3560.

[32] KISSINGER H E. Reaction kinetics in differential thermal analysis [J]. Analytical Chemistry, 1957, 29(11): 1702−1706.

[33] JONES L, DOLLIMORE D, NICKLIN T. Comparison of experimental kinetic decomposition data with master data using a linear plot method [J]. Thermochimica Acta, 1975, 13(2): 240−245.

[34] FANG Z Z, KANG X D, YANG Z X, WALKER G S, WANG P. Combined effects of functional cation and anion on the reversible dehydrogenation of $LiBH_4$ [J]. The Journal of Physical Chemistry C, 2011, 115(23): 11839−11845.

Ti 基添加剂对 Mg_2FeH_6 放氢性能的影响

徐晨晨，肖学章，邵 杰，刘朗夏，秦 腾，陈立新

浙江大学 材料科学与工程学院，硅材料国家重点实验室，
浙江省电池新材料与应用技术研究重点实验室，杭州 310027

摘 要：结合球磨和热处理制备掺杂 Ti，$TiMn_2$ 和 TiAl 的 Mg_2FeH_6 样品，并系统研究这些添加剂对 Mg_2FeH_6 样品放氢行为的影响。研究结果表明：所有添加剂都能够在一定程度上改善 Mg_2FeH_6 的放氢性能，特别是 $TiMn_2$ 对 Mg_2FeH_6 的放氢动力学性能改善效果显著。根据 Kissinger 方程计算出掺杂 $TiMn_2$ 的 Mg_2FeH_6 样品的放氢活化能为 94.87 kJ/mol，与未掺杂的 Mg_2FeH_6 样品相比，降低了 28 kJ/mol。另外，掺杂 $TiMn_2$ 的 Mg_2FeH_6 样品在循环测试过程中仍具有良好的放氢性能改善效果。

关键词：Mg_2FeH_6；Ti 基添加剂；放氢性能；动力学

(Edited by Mu-lan QIN)